Characterization of a Parallel-Stranded DNA Hairpin†

Markus W. Germann,‡ Hans J. Vogel,§ Richard T. Pon,‡ and Johan H. van de Sande*,‡

Department of Medical Biochemistry and Department of Biological Sciences, The University of Calgary, Calgary, Alberta, Canada T2N 4N1

Received February 14, 1989; Revised Manuscript Received April 17, 1989

ABSTRACT: Recently we have shown that synthetic DNA containing homooligomeric A-T base pairs can form a parallel-stranded intramolecular hairpin structure [van de Sande et al. (1988) *Science (Washington, D.C.) 241*, 551-557]. In the present study, we have employed NMR and optical spectroscopy to investigate the structure of the parallel-stranded (PS) DNA hairpin 3′-d$(T)_8C_4(A)_8$-3′ and the related antiparallel (APS) hairpin 5′-d$(T)_8C_4(A)_8$-3′. The parallel orientation of the strands in the PS oligonucleotide is achieved by introducing a 5′-5′ phosphodiester linkage in the hairpin loop. Ultraviolet spectroscopic and fluorescence data of drug binding are consistent with the formation of PS and APS structures, respectively, in these two hairpins. Vacuum circular dichroism measurements in combination with theoretical CD calculations indicate that the PS structure forms a right-handed helix. ^{31}P NMR measurements indicate that the conformation of the phosphodiester backbone of the PS structure is not drastically different from that of the APS control. The presence of slowly exchanging imino protons at 14 ppm and the observation of nuclear Overhauser enhancement between imino protons and the AH-2 protons demonstrate that similar base pairing and base stacking between T and A residues occur in both hairpins. However, the small chemical shift dispersion observed in proton NMR spectra of the PS hairpin suggests that the stem of this hairpin is more regular than that of the APS hairpin. On the basis of NOESY measurements, we find that the orientation of the bases is in the anti region and that the sugar puckering is in the 2′-endo range. Our results indicate a B-like conformation for each of the strands in the stem part of the PS hairpin and reverse Watson-Crick base pairing between the T and A residues. These data are consistent with a previously calculated structure for parallel-stranded DNA [Pattabiraman, N. (1986) *Biopolymers 25*, 1603-1606].

The potential existence of parallel-stranded double-helical structures of DNA and RNA has attracted some interest. Rich et al. (1961) reported that poly(A) could form a parallel-stranded duplex structure at low pH. More recent studies have demonstrated the formation of parallel-stranded duplex structures for the hexamer $d(T)_6$ containing methylated phosphate triesters (Koole et al., 1987) and for the duplex between α-deoxyoligonucleotides and the complementary β-deoxyoligonucleotides (Morvan et al., 1987; Thuong et al., 1987; Praseuth et al., 1987). The parallel-stranded nature of these oligo- and polynucleotides is a consequence of unusual chemical or environmental features not present in natural DNA. Pattabiraman (1986) suggested on the basis of molecular mechanics calculations that a parallel-stranded right-handed structure with reverse Watson-Crick-type base pairing is energetically as favorable as the conventional antiparallel form for the homooligomeric duplex $dA_6 \cdot dT_6$. In this predicted structure, the glycosidic torsion angles are anti, and the sugar conformation in each strand is similar to that of B-DNA.

We have recently provided evidence that oligodeoxyribonucleotides containing homooligomeric A-T base pairs can indeed form parallel-stranded duplexes (van de Sande et al., 1988). These parallel-stranded (PS)[1] structures were formed from deoxyoligonucleotides containing the complementary sequence $d(A)_{10} \cdot d(T)_{10}$ connected by a four-nucleotide hairpin loop with either a 3′-3′ or a 5′-5′ phosphodiester linkage. Parallel-stranded DNA is, however, not restricted to such special systems but can also be formed from conventional oligonucleotides with the appropriate sequence homology (Germann et al., 1988; Ramsing & Jovin, 1988). Therefore, the 5′-5′ or 3′-3′ phosphodiester linkage simply served to selectively stabilize intramolecular parallel-stranded DNA. The rather surprising thermal stability of the parallel-stranded hairpins, observed in these studies, indicated that homooligomeric structures with a smaller stem component would be sufficiently stable while at the same being a more suitable substrate for high-resolution NMR studies. In the present investigation, we have used proton NMR and other spectroscopic techniques to characterize the parallel-stranded DNA hairpin 3′-d$(T)_8C_4(A)_8$-3′ which contains a 5′-5′ phosphodiester linkage between the T and C residues. The results are compared to a control hairpin, 5′-d$(T)_8C_4(A)_8$-3′, which is devoid of this linkage and would therefore be expected to form a normal APS structure, with the stem resembling B-DNA as has been observed for other hairpin structures.

Materials and Methods

Materials. Oligodeoxynucleotides were synthesized by using automated phosphoramidite chemistry on a DNA synthesizer (Applied Biosystems Model 380A). 5′-Phosphoramidites were synthesized as described previously (van de Sande et al., 1988). The 3′-tritylated synthesis products were purified by re-

† Supported by the Medical Research Council of Canada and the Alberta Heritage Foundation for Medical Research (AHFMR). H.J.V. and M.W.G. are the holders of a scholarship and a studentship, respectively, of the AHFMR.

* Address correspondence to this author.
‡ Department of Medical Biochemistry.
§ Department of Biological Sciences.

[1] Abbreviations: APS, antiparallel stranded; bpb, bromophenol blue; CD, circular dichroism; DSS, 2,2-dimethylsilapentane-5-sulfonate; EDTA, ethylenediaminetetraacetic acid; HPLC, high-performance liquid chromatography; NOE, nuclear Overhauser effect; NOESY, nuclear Overhauser effect spectroscopy; PS, parallel stranded; UV, ultraviolet; xcff, xylene cyanol.

0006-2960/89/0428-6220$01.50/0

versed-phase HPLC[1] on a PRP-1 column (Germann et al., 1987), detritylated, and desalted on a Sephadex G-25 column. Molar extinction coefficients of the pure products were estimated from the extinction coefficients of the mononucleotides at 90 °C in 5 M $NaClO_4$ (Germann and van de Sande, unpublished results).

Hoechst 33258 was a gift from Dr. H. Loewe, Hoechst Laboratories, Frankfurt, West Germany, and netropsin was supplied by Lederle Laboratories, Pearl River, NJ. Extinction coefficients of 4.2×10^4 M^{-1} cm^{-1} at 338 nm (Hoechst 33258) and 2.1×10^4 M^{-1} cm^{-1} at 296 nm (Netropsin) were used (Latt & Wohlleb, 1975; Zimmer, 1973).

Optical Spectroscopy. Thermal denaturation profiles were recorded with a Varian 2280 spectrophotometer equipped with temperature-regulated cuvette holders.

Circular dichroism (CD) measurements were carried out on a Jasco J-500C spectropolarimeter equipped with a temperature control unit. For the vacuum CD measurements, samples were degassed by several freeze–thaw–pump cycles, and the cell compartment was flushed with N_2. Due to the strong absorbance of the buffer below 195 nm, a 1-mm cell and $MgCl_2$ were used in order to work at a low chloride ion concentration while still providing sufficient thermal stability.

Fluorescence measurements were obtained at 10 °C on a Perkin-Elmer 560-10S fluorescence spectrophotometer. The excitation and emission wavelengths were as follows: Hoechst 33258, λ_{ex} 355 nm, λ_{em} 480 nm; ethidium bromide, λ_{ex} 525 nm, λ_{em} 600 nm.

Thermal Denaturation Analysis. Thermally induced helix–coil transitions were monitored at 268 nm, using a temperature gradient of 0.5 °C/min. Absorbance readings were collected at 0.5 °C intervals and corrected for volume expansion. A concerted two-state model in which the absorbances of helix and coil forms were allowed to vary linearly with the temperature was employed to analyze the data (Pörschke & Jung, 1982). The measured absorbance was fitted to eq 1 using a Simplex procedure where A_T is the

$$A_T = A_H(1 - \Theta) + A_C\Theta \quad (1)$$

absorbance of the oligonucleotide as a function of temperature and A_H and A_C are the absorbances of helix and coil forms, respectively. The degree of transition (Θ) is given by [C]/([H] + [C]) where [C] and [H] represent the concentration of the oligonucleotide in the denatured and native forms, respectively. Entropies were calculated from $\Delta S° = \Delta H°_{vH}/T_M$, where $\Delta H°_{vH}$ is the van't Hoff enthalpy, R is the gas constant, and T_M is the melting temperature in degrees kelvin.

Calculation of the Circular Dichroism. Theoretical circular dichroism spectra of the stem part of the parallel and antiparallel DNA hairpins were calculated by using the quantum mechanical matrix method (Williams et al., 1986). The coordinates that were used for the stem structure of the APS structure were those of regular B-DNA (Arnott & Hukins, 1972). The coordinates for the PS stem structure were based on that of B-DNA except that a 180° rotation of thymine around the N_3–C_6 axis was implemented. The dielectric constant used in the calculations was 2.0.

NMR Spectroscopy. All NMR measurements were done on a Bruker AM-400 wide-bore spectrometer equipped with an Aspect 3000 computer. Proton-decoupled ^{31}P NMR data were recorded by using a 10-mm broad-band probe tuned to phosphorus (162 MHz). A gated two-level decoupling procedure was employed for proton decoupling. ^{31}P NMR samples were typically 0.2 mM strands in 1.7 mL of H_2O (10% D_2O) containing 50 mM Tris-HCl, 100 mM NaCl, and 0.1 mM EDTA, pH 7.0. The ^{31}P parameters were as follows: pulse length, 9 μs (50°); acquisition time, 1.4 s; relaxation delay, 3 s. Approximately 1000 scans were collected in 8K data sets. Chemical shifts are referenced to 85% phosphoric acid as an external standard at 10 °C and are given a negative sign when upfield from this standard.

^1H chemical shifts are referenced to internal DSS. Samples containing 6 or 210 A_{260} units were dissolved in 0.3 mL of 100 mM NaCl, 10 mM sodium phosphate, and 0.1 mM EDTA, pH 7.0 (ca. 0.4 or 2.5 mM in strands). Samples were repeatedly lyophilized from 99.9% D_2O and finally redissolved in 99.996% D_2O (MSD Isotopes) and transferred to 5-mm NMR tubes (Wilmad). Nonselective relaxation data were acquired at 15 °C by using a $(180°-\tau-90°-\text{observe})_n$ pulse sequence. Delay times (τ) between 0.4 and 10 s were used, and a 15-s relaxation delay was employed to ensure complete relaxation between scans. For each delay time, 32 scans were acquired in 16K data sets.

Imino proton spectra were recorded by using the jump and return pulse sequence (Plateau & Guéron, 1982). The parameters were as follows: the carrier was set at the water resonance, the spectral width was 10 000 Hz, and the acquisition time was 0.81 s. The delay between the phase-shifted pulses was 100 μs. Data were collected in 16K data sets. Samples containing 105 A_{260} units (ca. 2 mM in strands) were dissolved in 0.3 mL of 100 mM NaCl, 10 mM sodium phosphate, and 0.1 mM EDTA, pH 6.0, containing 10% D_2O.

Nuclear Overhauser effects from the imino to aromatic protons were measured at 15 °C by collecting sets of 8 or 16 scans with the decoupler alternately on- and off-resonance. Typically, a total of 800 scans were collected for each experiment. Imino protons were irradiated for 0.25–0.5 s with sufficient power to obtain 80% saturation. The relaxation delay between the experiments was 4 s, and the acquisition time was 0.41 s. The signal to noise ratio in the spectra was improved by applying a 5-Hz line-broadening contribution.

Saturation recovery data of the imino protons were obtained with a similar pulse sequence but with a 2-s irradiation and a delay between experiments of 4 s. The delay between the saturation pulse and the observation pulse was varied from 1 to 500 ms.

Two-dimensional phase-sensitive NOESY spectra were obtained at 20 °C using the time-proportional phase incremental method (Marion & Wüthrich, 1983). The spectral width in both dimension was 3500 Hz, and the carrier was set at the residual HDO peak. NOESY data sets of 2K were collected for each of the 512 t_1 values, with 64 scans per t_1. Mixing times of 80 and 250 ms and a relaxation delay of 2.3 s between experiments was used. The data were zero-filled in the t_1 dimension resulting in a 2K × 1K data matrix and multiplied by a 45°-shifted sine bell function.

Results and Discussion

Structures. The sequences of the two oligonucleotides studied are shown in Figure 1A,B. Both oligonucleotides can form either intramolecular hairpin structures or intermolecular dimeric structures. The monomer–dimer equilibrium of DNA hairpin structures is shifted to the intramolecular hairpin conformation at low DNA concentrations and high temperature, whereas the addition of salt favors the formation of the intermolecular dimer. Oligonucleotides containing built-in hairpin loops at the center of the sequence have a much lower tendency to give rise to a dimeric form, and as a consequence, hairpin structures predominate even at high strand concentrations (Haasnoot et al., 1980; Patel et al., 1982; Marky et al., 1983; Ikuta et al., 1986; Wolk et al., 1988). The PS oligonucleotide investigated in this study is designed to form

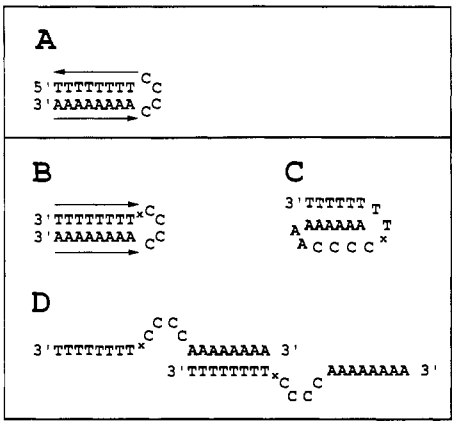

FIGURE 1: (A) Intramolecular antiparallel hairpin structure (APS). (B) Intramolecular parallel hairpin structure (PS). The location of the 5′–5′ internucleotide bond is indicated by x. (C) Possible intramolecular antiparallel clip structure for the PS oligonucleotide. (D) Possible intramolecular antiparallel (dimeric) structure for the PS oligonucleotide. This structure has the potential for forming concatamers.

Table I: Comparison of UV Difference Spectroscopic Data for Parallel-Stranded DNA Structures

	3′-$dT_8C_4A_8$-3′	3′-$dT_{10}C_4A_{10}$-3′[a]	dimeric[b]
isosbestic point (nm)	266	267	267
$\Delta\epsilon_{255nm}$	+0.8	+1.1	+1.5
$\Delta\epsilon_{280nm}$	−0.7	−0.6	−0.7

[a] van de Sande et al. (1988). [b] Germann et al. (1988).

an intramolecular parallel-stranded hairpin structure which by analogy to the parallel structures investigated previously is presumed to be less stable than the antiparallel control (van de Sande et al., 1988). It is therefore important to consider potential alternative structures for this sequence. The formation of a base-paired dimeric structure in a parallel conformation is very unlikely; however, a partially base-paired antiparallel dimeric structure could potentially form (Figure 1D). This dimer contains only 8 base pairs and is therefore not expected to be very stable, but it has the potential for forming concatamers at higher strand concentration. Dimeric and concatameric structures can be recognized by their concentration-dependent thermodynamic and spectroscopic properties. Concentration independence of the physical properties would be consistent with an intramolecular structure and would therefore indicate the formation of a parallel-stranded hairpin. Alternative antiparallel models, however, particularly for smaller oligonucleotides, will have to be considered (Figure 1C).

Characterization and Properties of PS and APS Hairpins. The PS and APS oligonucleotides were analyzed as described previously for $d(T)_{10}C_4(A)_{10}$ (van de Sande et al., 1988). Both PS and APS oligomers have similar gel electrophoretic mobilities under nondenaturing conditions and migrate exclusively as single bands, indicating that only intramolecular duplex structures (hairpins) were formed. The ultraviolet absorbance spectrum and hyperchromic behavior of the PS oligonucleotide are similar (see Table I) to those observed previously for both intra- and intermolecularly formed parallel-stranded structures. These optical properties are characteristic features of parallel-stranded DNA containing A-T base pairs (Germann et al., 1988; Ramsing & Jovin, 1988; van de Sande et al., 1988). Both the PS and the APS oligonucleotides undergo a thermally induced transition from a base-stacked double helix to a denatured coil form (Figure 2). For both structures, the salt-dependent transitions were monophasic and fully reversible

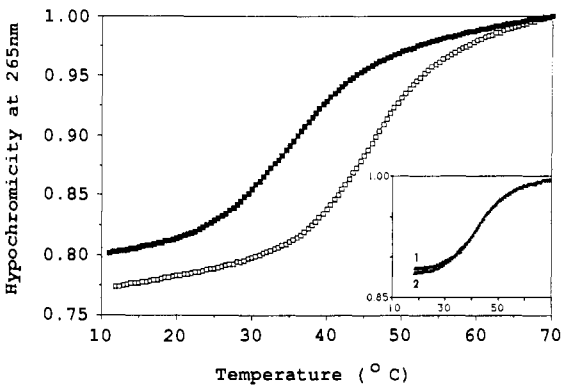

FIGURE 2: Thermal denaturation of PS (■) and APS (□) hairpin structures at a strand concentration of ca. 5.3 μM in 100 mM NaCl, 0.1 mM EDTA, and 10 mM phosphate, pH 7.0. The absorbance at 265 nm was monitored upon increasing or decreasing the temperature. Inset: Concentration independence of the thermal denaturation followed at 259 nm of the PS hairpin structure. ([1] = 120 μM, [2] = 3.8 μM in strands.)

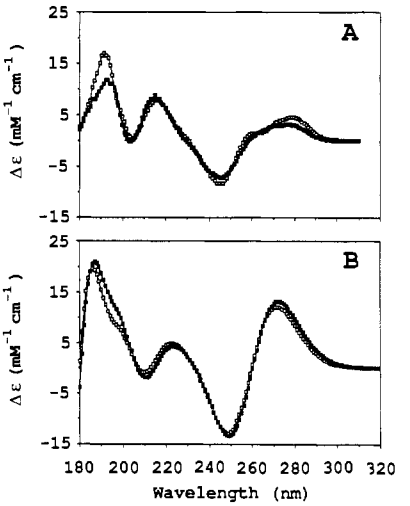

FIGURE 3: (A) Vacuum circular dichroism spectra of native PS (■) and APS (□) hairpin structures in 5 mM $MgCl_2$ and 10 mM Tris, pH 7.0 at 15 °C. (B) Calculated circular dichroism of native PS (■) and APS (□) hairpin structures. Δε is given per residue.

Table II: Thermodynamic Data for the Helix–Coil Transition of PS and APS DNA Hairpins

	5′-$dT_8C_4A_8$-3′		3′-$dT_8C_4A_8$-3′	
T_m (°C)[a]	45.6	(51.4)	35.2	(40.6)
$\Delta H°$ (kJ mol^{-1})	190	(248)	154	(205)
$\Delta h°$ (neighbor)	27.1	(27.6)	22.0	(22.8)
$\Delta S°$ (J mol^{-1} K^{-1})	596	(764)	500	(653)
$\Delta s°$ (neighbor)	85.1	(84.9)	71.4	(72.6)
ΔT_m (APS − PS)	10.5		(10.8)	

[a] Melting temperatures (T_m), $\Delta H°$ (van't Hoff enthalpy), and $\Delta S°$ (melting entropy) were determined in 0.1 M NaCl, 0.1 mM EDTA, and 10 mM sodium phosphate, pH 7.0. $\Delta h°$ and $\Delta s°$ are the enthalpy and entropy change per mole of nearest-neighbor interaction. Values in parentheses refer to $dT_{10}C_4A_{10}$.

and could be fitted to a two-state model (Table II). The concentration-independent melting behavior (Figure 2, inset) confirmed intramolecular duplex formation for the PS structure for strand concentrations up to 0.10 mM.

The circular dichroism for both DNA hairpins is shown in Figure 3A. Recent theoretical and experimental studies have shown that the circular dichroism at short wavelengths can serve as an indicator for the helical handedness of double-stranded nucleic acids (Sutherland et al., 1981; Williams et al., 1986). Right-handed helices with Watson–Crick-type base

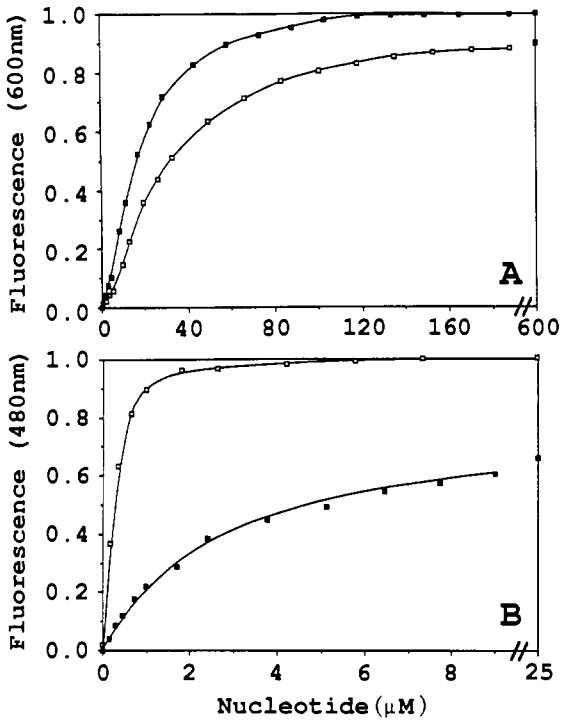

FIGURE 4: Drug binding to PS and APS hairpin. (A) Titration of 0.25 μM ethidium bromide in 100 mM NaCl, 0.1 mM EDTA, and 10 mM Tris, pH 7.0 at 10 °C, with PS (■) and (□) APS samples. (B) Titration of 20 nM Hoechst 33258, 400 mM NaCl, 0.1 mM EDTA, and 10 mM Tris, pH 7.0 at 10 °C, with PS (■) and APS (□) hairpins. The solid lines in (B) are model predictions based on a simple bimolecular reaction and the affinities given in the text. The measured fluorescence was normalized to 1 in both (A) and (B), and DNA concentrations are given per residue.

pairing show a positive peak in the "vacuum CD" between 180 and 200 nm. Although the PS hairpin shows a positive dichroism at that wavelength, it is important to assess the effects of the rotated thymines in the PS structure. We therefore calculated the theoretical CD spectra for a right-handed stem part of the APS (Watson–Crick) and PS (reverse Watson–Crick) hairpins (Figure 3B).[2] In both cases, a positive band at 190 nm is predicted. Both sets of spectra exhibit similar relative intensities for the PS and APS structure. The overall fit between theory and experiment indicates that a right-handed double-helical PS structure constructed from B-DNA helical parameters is compatible with the experimental data.[3] Large deviations in the calculated intensity occur above 260 nm. This region was noted previously to be very sensitive to the monomer transition data used for the calculation (Williams et al., 1986).

Drug–DNA Interactions. As was noted previously (van de Sande et al., 1988), parallel-stranded DNA is characterized by a nearly 2-fold fluorescence enhancement of the intercalator ethidium bromide compared to the antiparallel control at low DNA concentrations. This could be due to several possibilities: (1) the intercalator has an increased affinity for PS DNA; (2) the quantum yield of ethidium bromide bound to the PS structure is higher; or (3) the PS structure does not exhibit the nearest-neighbor exclusion-type binding observed for APS DNA. In order to distinguish between these possibilities, titration experiments were carried out (Figure 4A). The midpoints of the titration are at 1.6×10^{-5} and 2.6×10^{-5} M (in nucleotides) for the PS and APS hairpin, respectively. Upon increasing the DNA concentration, both binding curves reach a plateau, but the APS hairpin exhibits only a slightly lower fluorescence than the PS hairpin. Under these conditions, the concentration of the hairpins is more than 10-fold greater than the dye concentration, and therefore each hairpin would bind less than one dye molecule. The only apparent difference in the emission spectra, recorded at the end point of the titration, is the lower fluorescence intensity obtained for the APS structure. This is indicative of a lower quantum yield and demonstrates that variations at the intercalation sites are experienced by the reporter molecule. The difference in fluorescence, however, is too small to account for the nearly 2-fold fluorescence enhancement obtained at lower DNA concentrations. Thus, we conclude that the intercalator ethidium bromide binds stronger to parallel-stranded DNA.

The minor groove binding A-T specific drug Hoechst 33258 shows a drastically reduced fluorescence enhancement for the PS hairpin (Figure 4B). This drug exhibits two modes of binding to DNA: The low-affinity binding, which is insensitive to the base composition, is greatly reduced by increasing the ionic strength (Latt & Wohlleb, 1975) and shows a fluorescence emission at about 490 nm (Stokke & Steen, 1985). The high-affinity binding mode is sensitive to the base composition but is essentially independent of the salt concentration and exhibits an emission maximum at 460 nm. Both the PS and the APS hairpins display the spectral properties and the salt-independent binding (0.4–2.0 M NaCl) associated with the tight binding mode (data not shown). Footprinting studies have shown that this drug requires at least four consecutive A-T base pairs for specific binding (Jorgenson et al., 1988) and that it makes hydrogen bond contacts in the minor groove with the N3 of adenine and the O2 of thymine (Pjura et al., 1987). Consequently, each hairpin molecule can provide only a single binding site, and, therefore, the binding of the drug can be analyzed by using a simple bimolecular model. We have used Scatchard plots and curve fitting to calculate binding constants of $(8.1 \pm 0.4) \times 10^6$ and $(5.4 \pm 0.6) \times 10^8$ M^{-1} for the PS and APS hairpin, respectively.[4] The greatly reduced affinity of the PS hairpin for the drug suggests that the helical parameters of the PS structure are significantly different from those of B-DNA (van de Sande et al., 1988; Germann et al., 1988).[5]

[2] Our comparison of experimental and theoretical CD data is based on the premise that the loop structure contributes little to the CD. The loop contribution to the circular dichroism was assessed to be small, since both crossover points and peak maxima occur at the same wavelength for structures with 8 or 10 base pairs in the stem (van de Sande et al., 1988). If the loop structure contributed substantially to the CD, then this effect would be more pronounced for the smaller hairpin structure.

[3] PS models based on A-DNA parameters disagree markedly with the experimental data, although a positive band at 190 nm is also predicted.

[4] The strong binding observed to the APS structure could indicate that the drug is able to significantly stabilize dimeric or multimeric forms of the PS hairpin (see Figure 1C). However, binding curves obtained for the PS structure are not compatible with such a model, because it would be strongly dependent on the strand concentration and it would require that there is a large amount of dimeric or multimeric structures present even at low concentrations. In addition, we find that the equilibrium constant calculated at a 10-fold lower drug concentration does not differ from that at the higher drug concentration.

[5] The binding constant which was calculated here for the binding of Hoechst 33258 to the APS hairpin is larger than the range reported previously (10^6–10^7 M^{-1}) for polynucleotides with differing AT contents (Bontemps et al., 1975; Mikailov et al., 1981). We confirmed our data by a control experiment with poly(dA·dT). Both the polynucleotide and the APS hairpin bind the drug with similar affinity; thus, we conclude that the larger binding constant obtained for the APS hairpin is not due to structural peculiarities of this oligonucleotide. In addition, competition experiments with the strongly binding [$K_{eq} = (1–2) \times 10^9$ M^{-1}; Marky et al., 1984], minor groove specific drug netropsin show that Hoechst 33258 has only a 6–10-fold lower binding constant than this drug, which is again consistent with our results.

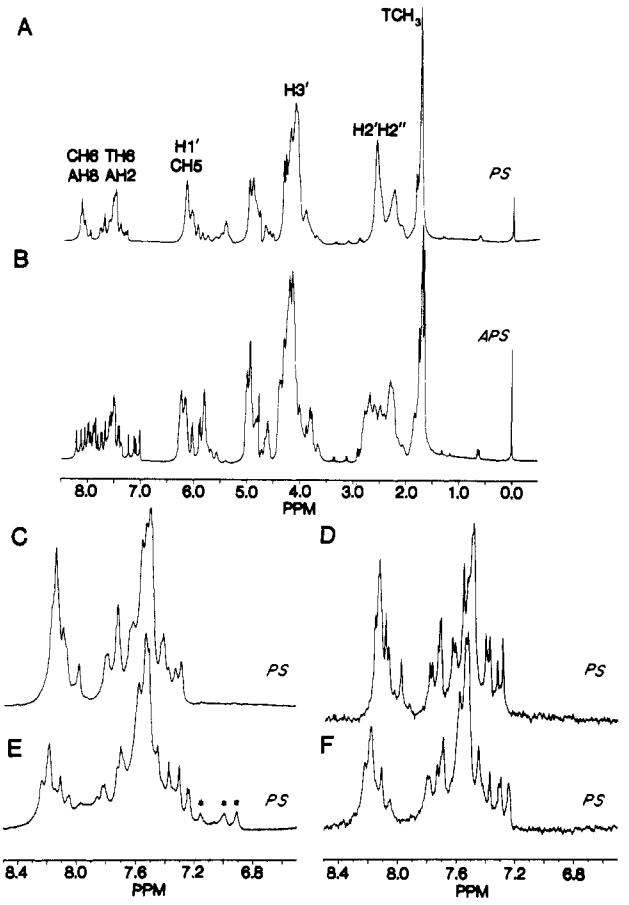

FIGURE 5: Proton NMR spectra (400 MHz) of PS and APS hairpin structures in 100 mM NaCl, 0.1 mM EDTA, and 10 mM phosphate, pH 7.0. (A) PS hairpin at 25 °C (900 A_{260} units/mL). (B) APS hairpin at 25 °C (900 A_{260} units/mL). (C) PS hairpin at 25 °C (900 A_{260} units/mL). (D) PS hairpin at 25 °C (19 A_{260} units/mL). (E) PS hairpin at 5 °C (900 A_{260} units/mL); resonances of the minor form are marked by an asterisk. (F) PS hairpin at 5 °C (19 A_{260} units/mL).

NMR of Parallel-Stranded DNA. Proton NMR spectra recorded for the PS and APS oligomers at temperatures above their melting points are similar as would be expected for oligonucleotides of the same base composition (data not shown). Spectra obtained for the native forms, however, differ considerably from the denatured forms and from each other (Figure 5A,B). Particularly striking is that the thymine methyl groups of the PS hairpin have a very similar chemical shift. The aromatic resonances of the PS structure also show a smaller degree of chemical shift dispersion than the APS control, indicating that the residues experience different ring current shifts in the two structures and that the PS hairpin possibly forms a structure which allows for fewer variations.

The high strand concentrations needed for the NMR experiments (50-fold higher than the ones used for the UV melting experiment) could promote the formation of intermolecular complexes. For example, the PS oligonucleotide could potentially form concatameric structures in the conventional antiparallel manner (Figure 1D). It is therefore important to demonstrate that the dominant species which is present under the NMR conditions is an intramolecular hairpin structure. NMR spectra obtained at low concentration (19 A_{260} units/mL), corresponding to the strand concentration at which the UV melting curve was measured, show the same features as those obtained at high concentration (900 A_{260} units/mL) (Figure 5C,D). In addition, the melting temperature determined from the chemical shift of the methyl groups corresponds to the T_M obtained from the UV melting study. This demonstrates that the higher strand concentration does not cause the formation of significant amounts of intermolecular (antiparallel) structures above 20 °C and, therefore, that the spectral characteristics are an intrinsic feature of the PS structure. Upon decreasing the temperature to 15 °C or lower, a small amount of a minor form (indicated by asterisk) becomes detectable in the high but not in the low concentration sample (Figure 5E,F). Raising the temperature to 20 °C results in the disappearance of this intermolecular form. These experiments suggest that an intermolecular complex can form in a reversible manner at high concentration and low temperature. However, conditions can be chosen such that the intramolecular form is highly preferred.

Phosphodiester Backbone Conformation. The ^{31}P chemical shift of phosphate esters in DNA is sensitive to a number of factors, the most prominent of these being the backbone torsion angles (Gorenstein et al., 1988). Thus, chemical shift information can be used to monitor helix–coil transitions and may also serve as an aid in classifying DNA structures into left-handed (Z) and right-handed (A, B) helices (Chen & Cohen, 1984). The phosphorus NMR spectra of the denatured PS and APS oligomers are shown in Figure 6A,B. Both spectra are similar as expected for random coils of the same base composition with the exception of the resonance at 1.0 ppm which is due to the unusual 5′–5′ phosphodiester linkage. A downfield-shifted 5′–5′ phosphodiester bond was also observed in r(CxUpG) where x indicates the location of the 5′–′5 linkage (Buchko, 1986). Spectra recorded under native conditions are upfield-shifted and are centered around −0.4 and −0.6 ppm for the PS and APS oligomer, respectively (Figure 6C,D). The chemical shifts observed for both native structures are in a region which is characteristic for right-handed helices (Chen & Cohen, 1984). This implies that the backbone conformation of the stem of the PS structure as judged from the ^{31}P chemical shift is not dramatically different from that of the control. On the basis of the slightly larger spread of the resonances of the PS hairpin and the segregation of the peaks into two main groups, one could speculate that slightly different conformations exist for the phosphodiester backbone in the A and T tract of this oligonucleotide. The two resolved resonances at 0.05 and −0.2 ppm observed for the native APS hairpin likely result from the phosphodiesters in the loop region.

Structural Details of Parallel-Stranded DNA. The sequence requirement for the formation of parallel-stranded DNA and the size requirement for a thermally stable structure result in overlap of resonances in the proton NMR spectra. This is compounded by the fact that the parallel-stranded hairpin, in contrast to the control, shows very little chemical shift dispersion. Although these experimental constraints have prevented us from accomplishing a complete sequence-specific assignment, much useful information can still be obtained from NOESY spectra. Particularly if it is obtained at a short mixing time (80 ms), such a spectrum is simplified in that only short distances give rise to cross-peaks and spin diffusion is only of minor importance (Ernst et al., 1987). The information gained from the NOESY spectrum may then be used to point out the salient features of parallel-stranded DNA and to compare the stem part of the parallel-stranded hairpin to A-, B-, or Z-DNA as was suggested recently (Cohen, 1987).

As a first step in the analysis, the glycosidic torsion angle (χ) of the stem residues of the PS and APS hairpins are considered. Relative to the ribose ring, the bases can adopt two main conformations, syn and anti. The former would give rise to NOESY cross-peaks because of the short H8–H1′

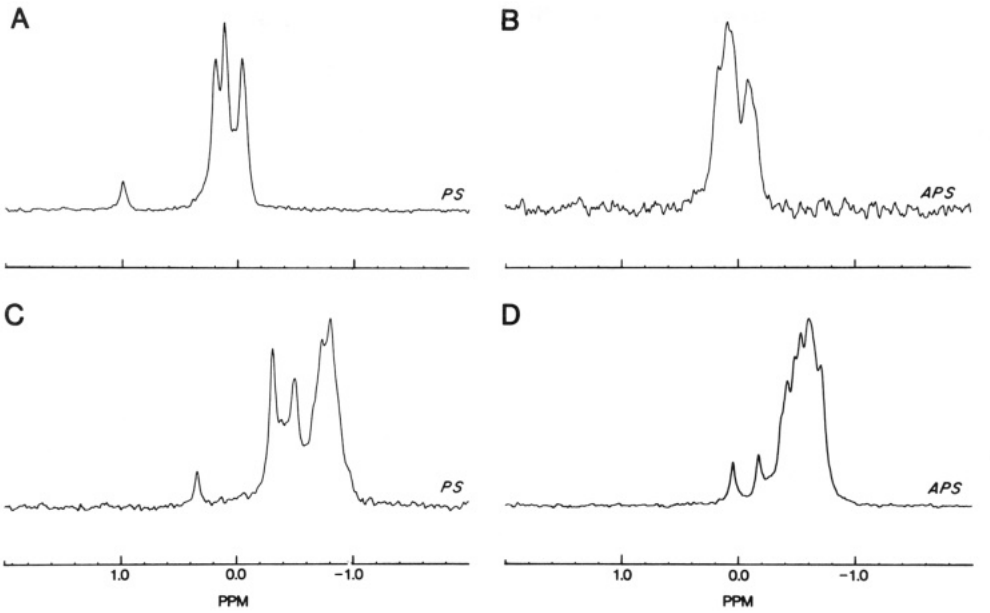

FIGURE 6: Phosphorus-31 NMR spectra (162 MHz) in 100 mM NaCl, 0.1 mM EDTA, and 50 mM Tris, pH 7.0. (A) PS hairpin at 70 °C. (B) APS hairpin at 70 °C. (C) PS hairpin at 10 °C. (D) APS hairpin at 10 °C.

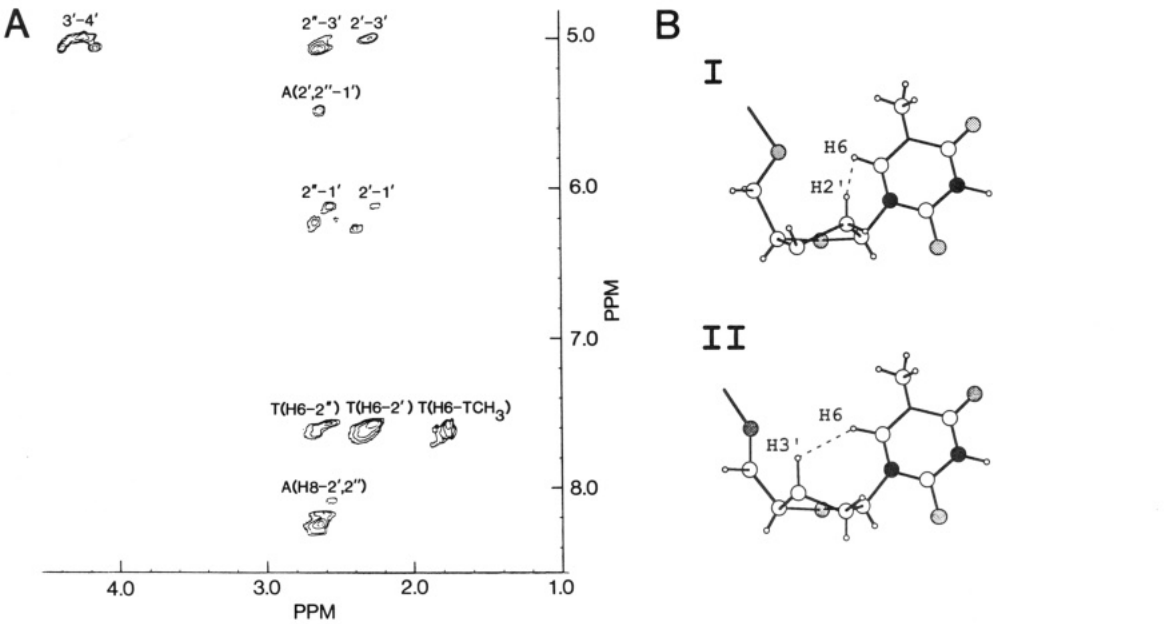

FIGURE 7: (A) Expanded contour plot of the phase-sensitive NOESY spectrum (mixing time 80 ms) of the PS hairpin in 100 mM NaCl, 0.1 mM EDTA, and 10 mM phosphate, pH 7.0 at 20 °C. (B) Characteristic short intranucleotide distances in A- and B-DNA. I: B-DNA (2′-endo sugar puckering), TH6–H2′. II: A-DNA (3′-endo sugar puckering), TH6–H3′.

distance (2.2 Å). In contrast, for a nucleotide in the anti range, this distance is typically 3.7 Å. Consequently, nucleotides in the syn conformation such as the G residues in Z-DNA always show a strong NOESY cross-peak for the G(H8–H1′) protons (Mirau & Kearns, 1984; Cohen, 1987). Both the PS and the APS oligonucleotides do not show cross-peaks for the A(H8–H1′) and the T(H6–H1′) protons in the 80-ms NOESY spectrum. The observation of cross-peaks for C(H5–H6) (2.4 Å) demonstrates that distances in that range can be readily detected under our experimental conditions (Figure 7A). We notice, however, strong cross-peaks between A(H8–H2′,2″) and T(H6–H2′,2″) which have been observed for A- and B-DNA where the bases are in the anti conformation (Mirau & Kearns, 1984; Cohen, 1987). The glycosidic torsion angles of the A and T residues in the PS structure are therefore clearly not compatible with a syn conformation, and our results suggest that they are in an anti orientation as in the APS structure.

The sugar conformation of parallel-stranded DNA can also be assessed from the NOESY spectrum, which for the PS oligonucleotide is characterized by an extensive overlap of the cross-peaks. Strong cross-peaks between base protons and deoxyribose protons are only observed for T(H6–H2′, H6–H2″), T(H6–TCH_3), and A(H8–H2′,2″) interactions in the stem part of the hairpin structure (Figure 7A). A similar cross-peak pattern was also obtained for the APS hairpin. The PS structure was analyzed by comparing its cross-peak pattern to those of A- and B-DNA, both of which are characterized by short intra- and internucleotide distances which give rise to characteristic NOESY spectra for both forms (Mirau & Kearns, 1984; Cohen, 1987, Wüthrich, 1986). In B-DNA (2′-endo conformation), the intranucleotide distances T(H6–

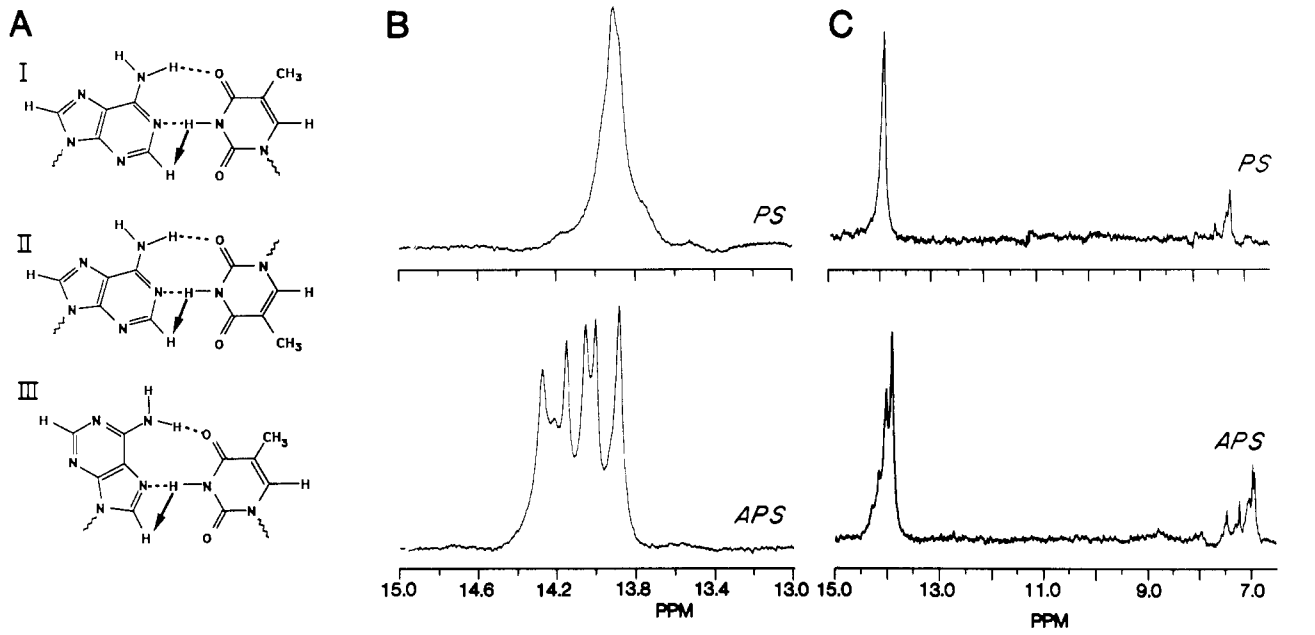

FIGURE 8: (A) Base pairing schemes. I: Watson–Crick. II: Reverse Watson–Crick. III: Hoogsteen-type base pairings. Arrows indicate NOE effects expected upon irradiating the thymine imino proton for each base pairing scheme. (B) Imino proton spectra of PS (top) and APS (bottom) hairpins in 100 mM NaCl, pH 6.0, recorded at 25 °C, using the jump and return pulse sequence. (C) 1D NOE difference spectra of PS (top) and APS (bottom) DNA (15 °C, 100 mM NaCl, pH 6.0). Imino protons were irradiated for 0.25 s. The AH-2 protons were identified from their characteristic slow relaxation behavior (Broido et al., 1985) in inversion recovery experiments. These assignment were independently confirmed from our NOESY data (both in D_2O).

H2′) and A(H8–H2′) are short (2.4 and 2.0 Å) while for an A-DNA (3′-endo conformation) these distances are longer (~4 Å), (Figure 7B). However, due to the extensive overlap of the cross-peaks, internucleotide distances between T(H6–H2′) and A(H8–H2′) must be considered also. These distances are large (3.8 and 4.0 Å) in B-DNA but are short in A-DNA (2.1 and 2.0 Å). A distinction between 2′-endo and 3′-endo sugar puckering can therefore not be made on the basis of our NOESY data for T(H6–H2′) and A(H8–H2′) protons. In addition, the H2′ and H2″ resonances of the A residues also overlap extensively. The intranucleotide T(H6–H3′) and A(H8–H3′) distance can also be used as an indicator for the sugar puckering and is in our case more suitable (Figure 7B). Both intra- and internucleotide distances between T(H6–H3′) and A(H8–H3′) are short in A-DNA (2.5–3 Å) while in B-DNA these distances are considerably larger (>4 Å) and should not give rise to cross-peaks. Thus, the absence of this interaction indicates that the sugar puckering is in the 2′-endo range in both the A and T tracts of the PS structure. The observation of strong cross-peaks for the T(H6–H2″) protons in the PS hairpin is in agreement with our deduction, since in A-DNA both the intra- and intermolecular distances between those protons are large whereas in B-DNA both are considerably shorter. Further support is obtained from the absence of the H2″–H4′ cross-peak which would be expected for A-DNA (2.3 Å) but not for B-DNA. As was noted previously, strong cross-peaks are observed for T(CH_3–H6) and for H4′–H3′ protons corresponding to distances in the range of 2.5–2.9 Å.

Base Pairing in Parallel-Stranded DNA. The observation of imino protons for the PS hairpin with similar chemical shift as the APS hairpin demonstrates that base pairing and base stacking occur in the PS structure (Figure 8B). Imino protons of the PS structure are again less resolved than for the APS hairpin and are sensitive to temperature, disappearing below the melting point. The chemical shift of the PS imino protons indicates that they have a similar environment as the APS imino protons. We note that because of the symmetry of the thymine base, hydrogen bonds formed between the A-T base pairs are of the same type in a Watson–Crick or a reverse Watson–Crick base pair (Figure 8A). Reverse Watson–Crick and Watson–Crick basee pairing can be distinguished from Hoogsteen base pairing by a simple one-dimensional experiment in which the low-field thymine imino resonances are irradiated and changes in the aromatic region of the spectra are monitored (Assa-Munt & Kearns, 1984). At short irradiation times, only the AH-2 resonances exhibit an NOE (Figure 8C). This demonstrates that for both structures these protons must be close in space and are thus compatible with Watson–Crick or reverse Watson–Crick but not with Hoogsteen-type base pairing. This finding is also supported by chemical modification studies (van de Sande et al., 1988). On the basis of these experiments, a distinction between Watson–Crick or reverse Watson–Crick base pairing cannot be made, but we note that the dyad symmetry associated with Watson–Crick base pairing is not compatible with parallel-stranded duplexes (Saenger, 1984).

Presaturation experiments carried out in H_2O showed that at 20 °C only the antiparallel structure had any intensity left in the imino proton region, indicating faster exchange for the PS structure (data not shown). Saturation recovery measurements at 15–35 °C confirmed that the exchange rates for the PS hairpin (Figure 9) are 6–8 times faster than for the APS hairpin. The half-life times at 25 °C are 15 ms for the PS and 76 ms for the APS hairpin, which is consistent with the lower stability of the PS hairpin, and both show a similar temperature dependence. These values correspond to the overall exchange under our experimental conditions and are not a reflection of the actual helix opening rates since this requires extrapolation to high buffer concentration (Leroy et al., 1985).

CONCLUSION

The gel electrophoretic behavior, combined with the concentration independence of the thermal denaturation (Figure 2) and the NMR spectra (Figure 5C,D), rules out intermo-

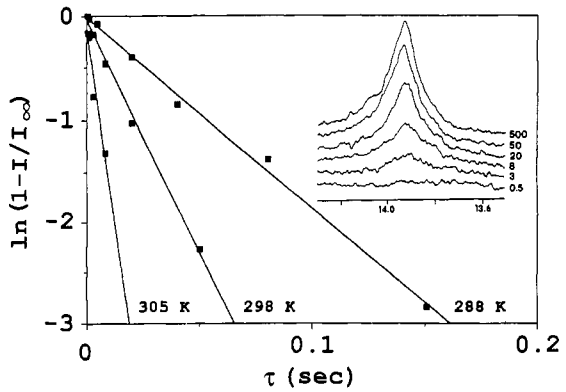

FIGURE 9: Saturation recovery of the imino protons of the PS hairpin structure. Imino protons were irradiated for 2 s with sufficient power to obtain 80–90% saturation of the resonances. Data were plotted for the first-order reaction $I = I_0(1 - e^{-k\tau})$ where I is the intensity of the imino proton resonance at delay τ and k is the rate constant for the exchange. The inset shows the spectra recorded at 25 °C for delay times of 0.5–500 ms between saturation and observation pulses.

lecular forms and shows that the PS oligonucleotide forms an intramolecular parallel-stranded hairpin structure. An alternative, antiparallel intramolecular structure (clip structure, Figure 1C) was rejected for the following reasons: (1) The small ^{1}H chemical shift dispersion observed for methyl and aromatic protons is not compatible with such a structure because some T (and A) residues would be part of the loop and therefore experience a different chemical environment. Also, the presence of such a loop structure would create a different environment for those residues in its vicinity and should result in different chemical shifts. This is also supported by the observation that the imino protons in the PS structure have very similar chemical shifts. (2) The length independence of the thermodynamic data strongly argues against the clip structure, since the formation of such a structure should show a distinct dependence upon the number of A-T base pairs. For shorter oligonucleotides (with 5–6 base pairs), the loop structure could be relatively small due to the positioning of the ends to be joined on the same side of the helix and also because of a smaller stem structure. Yet we find that the thermodynamic data are length independent and that the spectroscopic properties for both the 20-nt and 24-nt hairpin structures are strikingly similar (Tables I and II). (3) Intercalation of ethidium bromide is expected to destabilize the clip structure because of the increased end to end separation, and this should lead to a weaker binding; however, we find that the PS oligonucleotide has a higher affinity for the drug. In addition, the thermal stability of the PS hairpin is not affected by the presence of the drug. Thus, our data are fully consistent with an intramolecularly formed parallel-stranded DNA hairpin.

The helical handedness of the PS hairpin, as assessed by theoretical and experimental vacuum circular dichroism, is compatible with the experimentally observed spectra of a right-handed structure. In addition, we have investigated the helical parameters of the novel PS form by NMR. The phosphodiester backbone conformation appears to be similar to that of right-handed A- or B-type DNA as judged from the ^{31}P chemical shift. We have also analyzed the conformation of the PS oligonucleotide by comparison of the observed NOESY cross-peak pattern to those observed for A-, B-, or Z-DNA. We find that the bases in the stem are in an anti position and that the sugar puckering is in the 2′-endo range. The observation of NOE effects between T imino protons and AH-2 protons demonstrates that base pairing between these residues occurs in either Watson–Crick or reverse Watson–Crick, but not Hoogsteen, orientation. Since Watson–Crick-type base pairing is not compatible with the formation of parallel-stranded duplex DNA, we conclude that the base pairing occurs in the reverse Watson–Crick orientation as predicted by Pattabiraman (1986).

The chemical shifts of the stem residues in the PS structure are very similar as exemplified by the extensive overlap in the NOESY spectrum. This indicates a highly regular structure and points to an inability of PS DNA to accommodate substantial structural variation. We note that in B-type DNA and in PS DNA, obtained in a model by a 180° rotation of the T residues about the N_3–C_6 axis, the distances between the N9 of successive adenines or the N1 of successive thymines remain essentially preserved. In contrast, if the base pair is substantially displaced from the helical axis, major conformational changes in the backbone would be necessary to allow the formation of the PS DNA. This would seem unlikely considering the normal conformation of the sugar and phosphate backbone as judged by NMR. It will therefore be of interest to see whether the conformationally more conservative RNA can meet the PS structural requirements.

ACKNOWLEDGMENTS

We are indebted to Dr. N. Zhou, Dr. N. Pattabiraman, and B. W. Kalisch for constructive suggestions and assistance during the preparation of the manuscript. We also thank C. C. Hardin and C. Cheong for the CD program.

REFERENCES

Arnott, S., & Hukins, D. W. L. (1972) *Biochem. Biophys. Res. Commun. 47*, 1504–1509.

Assa-Munt, N., & Kearns, D. R. (1984) *Biochemistry 23*, 791–796.

Bontemps, J., Houssier, C., & Fredericq, E. (1975) *Nucleic Acids Res. 2*, 971–984.

Broido, M. S., James, T. L., Zon, G., & Keepers, J. W. (1985) *Eur. J. Biochem. 150*, 117–128.

Buchko, G. W. (1986) Thesis, McMaster University, Hamilton, Ontario.

Chen, C.-W., & Cohen, J. S. (1984) in *Phosphorus-31 NMR Principles and Applications* (Gorenstein, D., Ed.) pp 233–263, Academic Press, Orlando.

Cohen, J. S. (1987) *Trends Biochem. Sci. 12*, 132–135.

Ernst, R. R., Bodenhausen, G., & Wokaun, A. (1987) in *Principles of Nuclear Magnetic Resonance in One and Two Dimensions*, Clarendon, Oxford.

Germann, M. W., Pon, R. T., & van de Sande, J. H. (1987) *Anal. Biochem. 165*, 399–405.

Germann, M. W., Kalisch, B. W., & van de Sande, J. H. (1988) *Biochemistry 27*, 8302–8306.

Gorenstein, D. G., Schroeder, S. A., Fu, J. M., Metz, J. T., Roongta, V., & Jones, C. R. (1988) *Biochemistry 27*, 7223–7237.

Haasnoot, C. A. G., den Hartog, J. H. J., de Rooij, J. F. M., van Boom, J. H., & Altona, C. (1980) *Nucleic Acids Res. 8*, 169–181.

Ikuta, S., Chattopadhyaya, R., Dickerson, R. E., & Kearns, D. R. (1986) *Biochemistry 25*, 4840–4849.

Jorgenson, K. F., Varshney, U., & van de Sande, J. H. (1988) *J. Biomol. Struct. Dyn. 5*, 1005–1023.

Koole, L. H., van Genderen, M. H. P., & Buck, H. M. (1987) *J. Am. Chem. Soc. 109*, 3916–3921.

Latt, S. A., & Wohlleb, J. C. (1975) *Chromosoma (Berlin) 52*, 297–316.

Leroy, J. L., Broseta, D., & Guéron, M. (1985) *J. Mol. Biol. 184*, 165–178.

Marion, D., & Wüthrich, K. (1983) *Biochem. Biophys. Res. Commun. 113*, 957–974.
Marky, L. A., Blumenfeld, K. S., Kozlowski, S., & Breslauer, K. J. (1983) *Biopolymers 22*, 1247–1257.
Marky, L. A., Currey, J., & Breslauer, K. J. (1984) in *The Molecular Basis of Cancer* (Rein, R., Ed.) Liss, New York.
Mikhailov, M. V., Zasedatelev, A. S., Krylov, A. S., & Gurskii, G. V. (1981) *Mol. Biol. (Engl. Transl.) 15*, 541–554.
Mirau, P. A., & Kearns, D. R. (1984) *Biochemistry 23*, 5439–5446.
Morvan, F., Rayner, B., Imbach, J.-L., Lee, M., Hartley, J. A., Chang, D.-K., & Lown, J. W. (1987) *Nucleic Acids Res. 15*, 7027–7044.
Patel, D. J., Kozlowski, S. A., Ikuta, S., Itakura, K., Batt, R., & Hare, D. R. (1982) *Cold Spring Harbor Symp. Quant. Biol. 47*, 197–206.
Pattabiraman, N. (1986) *Biopolymers 25*, 1603–1606.
Pjura, P. E., Grzeskowiak, K., & Dickerson, R. E. (1987) *J. Mol. Biol. 197*, 257–271.
Plateau, P., & Guêron, M. (1982) *J. Am. Chem. Soc. 104*, 7310–7311.
Pörschke, D., & Jung, M. (1982) *Nucleic Acids Res. 10*, 6163–6176.
Praseuth, D., Chassigno, M., Takasugi, M., Doan, T. L., Thuong, N. T., & Hélène, C. (1987) *J. Mol. Biol. 196*, 939–942.
Ramsing, N. B., & Jovin, T. M. (1988) *Nucleic Acids Res. 14*, 6659–6676.
Rich, A., Davies, D. R., Crick, F. H., & Watson, J. D. (1961) *J. Mol. Biol. 3*, 71–86.
Saenger, W. (1984) in *Principles of Nucleic Acid Structure*, Springer Verlag, New York.
Stokke, T., & Steen, H. B. (1985) *J. Histochem. Cytochem. 33*, 333–338.
Sutherland, J. C., Griffin, K. P., Keck, P. C., & Takacs, P. Z. (1981) *Proc. Natl. Acad. Sci. U.S.A. 78*, 4801–4804.
Thuong, N. T., Asseline, U., Roig, V., Takasugi, M., & Hélène, C. (1987) *Proc. Natl. Acad. Sci. U.S.A. 84*, 5129–5133.
van de Sande, J. H., Ramsing, N. B., Germann, M. W., Elhorst, W., Kalisch, B. W., Kitzing, E. V., Pon, R. T., Clegg, R. C., & Jovin, T. M. (1988) *Science (Washington, D.C.) 241*, 551–557.
Williams, A. L., Jr., Cheong, C., Tinoco, I., Jr., & Clark, L. B. (1986) *Nucleic Acids Res. 14*, 6649–6659.
Wolk, S. K., Hardin, C. C., Germann, M. W., van de Sande, J. H., & Tinoco, I., Jr. (1988) *Biochemistry 27*, 6960–6967.
Wüthrich, K. (1986) *NMR of Proteins and Nucleic Acids*, Wiley, New York.
Zimmer, C. (1975) *Prog. Nucleic Acid Mol. Biol. 15*, 285–318.